Three-dimensional reconstruction of irregular foodstuffs

Sandro M. Goñi, Emmanuel Purlis, Viviana O. Salvadori

PII: S0260-8774(07)00181-1
DOI: 10.1016/j.jfoodeng.2007.03.021
Reference: JFOE 4875

To appear in: *Journal of Food Engineering*

Received Date: 28 November 2006
Revised Date: 12 February 2007
Accepted Date: 5 March 2007

Please cite this article as: Goñi, S.M., Purlis, E., Salvadori, V.O., Three-dimensional reconstruction of irregular foodstuffs, *Journal of Food Engineering* (2007), doi: 10.1016/j.jfoodeng.2007.03.021

Three-dimensional reconstruction of irregular foodstuffs

Sandro M. Goñi[a,b], Emmanuel Purlis[a], Viviana O. Salvadori[a,c *]

[a]Centro de Investigación y Desarrollo en Criotecnología de Alimentos (CIDCA), Facultad de Ciencias Exactas, UNLP-CONICET, 47 y 116, (B1900AJJ) La Plata, Argentina

[b]Depto. de Ciencia y Tecnología, UNQ, Bernal, Argentina

[c]MODIAL, , Depto. de Ing. Química, Facultad de Ingeniería, UNLP, La Plata, Argentina

Abstract

3-D reconstruction of general solid food materials was performed using a reverse engineering method based on a surface cross-sectional design. Digital images of cross-sections of irregular multi-dimensional foodstuffs were acquired using a computer vision system, and image processing was performed to obtain the actual boundaries. These boundaries were then approximated by closed B-Spline curves, which were assembled through a lofting technique to construct a geometrical representation of food materials. Considering the reconstructed objects, a procedure based on finite element method was developed to estimate the surface area and volume. The developed finite element method approach was validated against experimental volume values of apples and meat pieces, obtaining an estimation error less than 2%. Surface area prediction equations were proposed from estimated surface area values and weight and volume measurements. Good agreement was found with previously reported results.

Keywords: Lofting; B-Spline curves; Irregular shape; Surface area.

* Corresponding author. Tel./fax: +54 221 425 4853. *E-mail address:* vosalvad@ing.unlp.edu.ar (V. O. Salvadori).

1. Introduction

Many food engineering processes, especially, those including transfer phenomena and quality evaluation, involve measurement or estimation of the surface area and volume of food materials. For example, it is well known that heat and mass transfer coefficients depend on the shape and surface area of the object being analyzed In addition, volume dependent properties, like density, would be easily determined if the volume was correctly measured or estimated. Therefore, estimation of surface area and volume is an essential issue in the food engineering field. However, it is a tedious and difficult task, moreover, when irregular shaped objects are involved. Since many of food materials like grains, fruits and vegetables are approximately ellipsoidal in shape, some researchers worked on the development of an accurate and simple equation for the estimation of the surface area for such cases (Igathinathane & Chattopadhyay, 1998a,b, 2000; Kumar & Mathew, 2003; Somsen, Capelle, & Tramper, 2004; Taylor, Garboczi, Erdogan & Fowler, 2006). On the other hand, not many articles concerning shape analysis and estimation of surface area and volume regarding irregular three-dimensional foodstuffs had been published.

Clayton, Amos, Banks and Morton (1995) worked on the estimation of surface area of apples of four different cultivars. They applied various methods: sphere and ellipsoid analogies; correlation between actual surface area (estimated by tape method) and both fruit mass and volume; and the finite element method (FEM). The calculation of surface area using FEM was based on a computer software package developed previously (Cleland, Cleland, Earle & Byrne, 1984). In such method, a two-dimensional axisymmetrical coordinate grid depicting the shape of the fruit is formed. Surface area is then calculated based on this grid (Clayton et al., 1995). FEM was the most accurate of the numerically based methods that were evaluated.

Some work was done regarding shape description, but not including neither solid reconstruction nor surface area and volume estimation. For instance, with the aim of evaluating chilling time related shape factors, a three-dimensional laser scanning technique was used to digitize the surface of several types of meat cuts (Crocombe, Lovatt & Clarke, 1999). Three-dimensional surface data were collected from each meat cut and a bicubic Hermite surface model was then fitted to each data set to give a full mathematical description of the surface. From such models, Crocombe et al. (1999) determined the geometric shape factors used in the prediction of chilling, freezing and thawing times. In addition, following the objective of classifying and quality grading fruits, different shape descriptors were applied. Fourier descriptors were used to characterize the apple shape via the contour of digitized cross-sections that were obtained by image analysis (Currie, Ganeshanandam, Noiton, Garrick, Shelbourne & Oraguzie, 2000). Concerning three-dimensional shape description, Ding, Nesumi, Takano and Ukai (2000) worked on *Citrus* species using spherical harmonic descriptors; Beyer, Hahn, Peschel, Harz and Knoche (2002) described fruit shape in sweet cherry using image analysis and standard software.

Sabliov, Boldor, Keener and Farkas (2002) developed an image processing based method to measure volume and surface area of ellipsoidal agricultural products (eggs, lemons, limes and peaches). The method assumes that each product has an axisymmetric geometry and is a sum of superimposed elementary frustums of right circular cones. The product volume and surface area are calculated as the sum of the volumes and surface areas of individual frustums. Lee, Eifert, Zhan and Westover (2003) developed a computer vision technique combining laser triangulation and a distance transform to improve the 3-D measurement accuracy obtained by only applying laser triangulation, for objects with irregular shapes. Eifert, Sanglay, Lee, Sumner and Pierson (2006) utilized a machine vision system using radial projection technique (Lee, Xu, Eifert & Zhan, 2006) to measure the surface area of fresh foods: apples, cantaloupes, strawberries and tomatoes. A sequence of 30 images taken at the same angular interval was recorded for image processing for an object. Each image was treated as a slice of the cross-section of the object taken at a specific angular position. Then, location of boundary points on each image slice was extracted to create a 3-D wire-frame model for surface area estimation by commercial software. Finally, they proposed prediction equations for the surface area of each food shape from weight measurement. More recently, Zheng, Sun and Du (2006), and Du and Sun (2006) developed image processing techniques to estimate the surface area and volume of beef joints and hams, respectively. In both works, shape of samples was fitted to ellipsoidal geometry. Surface area and volume calculations were based on the concept of summing a finite number of regular conical sections, which axis were obtained through computer vision.

State of the art shows that previous articles were focused on estimation of surface area, or shape description of objects, having relatively high sphericity or being symmetrical in some way. However, most of foodstuffs do not present these geometrical properties. Therefore, there is an absence of accurate methods to estimate the surface area of food materials with arbitrarily irregular shapes. The overall objective of the present work is to simulate food preservation processes in irregular three-dimensional domains. To achieve this objective, it is first necessary to develop a method to obtain an irregular 3D representation of the real shape of foodstuffs. This paper presents the results of geometry modelling obtained by reverse engineering techniques.

Furthermore, a procedure based on finite element method was developed to estimate the surface area and volume of irregular food materials. The application of the resulting object reconstruction will be used as domain in simulation of preservation processes, which will be discussed in a future work

2. Method description

Reverse engineering is a technology to establish CAD (Computer Aided Design) geometry models from samples, prototypes, moulds or manufactured parts by digitization. A CAD technique called "skinning" or "lofting" could be employed for the reverse engineering applications (Lin, Liou & Lai, 1997). Skinning is a special case of cross-sectional design of surfaces (Piegl, 1991). Briefly, surface skinning is a process of passing a smooth surface through a set of so called cross-sectional curves (Piegl & Tiller, 1996). The most used mathematical description of free-shaped curves and surfaces is the well-known Non-Uniform Rational B-Splines (NURBS) representation (Moustakides, Briassoulis, Psarakis & Dimas, 2000). For further information about cross-sectional design, the reader should be referred to Woodward (1987, 1988).

2.1. Object reconstruction

Object reconstruction is a computational representation of the real food material geometry in its actual dimensions. The entire method was implemented in MATLAB® and COMSOL Multiphysics™ (version 3.2). The basic steps are described in the follows:

1. An axis was manually selected, along which the object would be sliced, by simple visual inspection. The sectioning axis was mainly chosen in order to obtain filled regions without interior holes, that is, to capture an image with a single closed boundary. Also, this axis should correspond to the direction presenting the minor irregularity of the object.

2. Sample sectioning was performed along the selected axis using a mechanical cut apparatus to ensure a controlled width for each section. The width of slices depends on the size and shape variability of the sample along its sectioning axis. That is, as more irregular is the sample, thinner slices must be taken to improve the approximation to the real shape. Afterwards, the sample was reconstructed by manually assembling the cut slices. Thus, the original spatial orientation and alignment of the samples was respected, which is essential for computational reconstruction accuracy.

3. Acquisition of images was done using a computer vision system (CVS), i.e. a PC equipped with a digital camera. The images were taken using a white or black background plate, depending on the sample colour. Choosing background colour is important in order to perform efficient boundary detection: as more contrast between sample and background is obtained, a better procedure of sample contour extraction will be done. Acquisition was performed as follows: the background plate was placed between the first and second slices, and the lens was situated orthogonally to the first slice. Therefore, the first slice was "isolated" from the entire sample without losing the original alignment. After image recording, the first slice was extracted and the background plate was placed between the second and third slices. This procedure was repeated until image of each slice was recorded.

4. The irregular contour was extracted from the images of slices, as follows:

4.1. Conversion of original RGB images to grey-scale format.

4.2. Noise reduction through a 3 x 3 median filter to enhance image quality.

4.3. Segmentation through a threshold value which was obtained analyzing the grey-scale image histogram. A binary image was obtained where black colour (pixel value equal to 0) represented the background and white colour the slice (pixel value equal to 1).

4.4. Boundary detection and interpolation of a subset of boundary pixels by a closed B-Spline curve (a continuous approximation to the discrete boundary of binary images).

Finally, the B-Spline curves representing the real boundaries of slices were correctly assembled by means of a lofting technique in COMSOL Multiphysics: a closed NURBS surface was constructed through B-Spline cross-section curves. The resulting surface was then transformed in a 3D solid object. It is worth to note that the number of segments of each B-Spline curve must be the same in all extracted boundaries to perform lofting. For further information about lofting technique implemented in COMSOL Multiphysics, the reader should be referred to COMSOL Multiphysics User's Guide.

A conversion factor, computed from a reference object, was used to convert the object dimensions from pixels to SI units during the image acquisition stage. The computational representation of the food material may be used to estimate its surface area and volume (see section 2.2), and as a geometry model in an engineering process modelling and simulation (and eventual optimization).

2.2. Surface area and volume estimation

A FEM approach method was developed to estimate the volume and surface area of reconstructed foodstuffs. These determinations, together with visual results, can be used to assess the reconstruction accuracy. The FEM approach method consists in approximating the surface area and volume of real foodstuffs as a sum of such properties of finite elements obtained by meshing the reconstructed object. Firstly, a mesh was generated using curved mesh elements to make the best approximation to the irregular shape. These elements are distorted simplices (tetrahedrons) that can approximate the boundary better than ordinary, straight mesh elements (COMSOL Multiphysics). In other words, the mesh elements are curved at the boundary, and thus come closer to the true geometric boundary. Delaunay algorithm was used to generate the mesh, which size and number of elements is determined by various properties such as maximum element size and curvature mesh size. These parameters are directly related to time calculation and computer capability, i.e. as more finer the mesh is, more time and PC memory are needed

Secondly, a general variable (u) was set equal to one in all mesh nodes. This is equivalent to solve a partial differential equation (PDE) which solution would be $u = 1$. Thirdly, a numerical integration for u was made over all boundary (Γ_i) and domain (Ω_i) elements to obtain the estimated surface area and volume values, respectively (Eq. (1)-(2)).

$$\tilde{S} = \sum_i \iint_{\Gamma_i} u \, d\Gamma_i \tag{1}$$

$$\tilde{V} = \sum_i \iiint_{\Omega_i} u \, d\Omega_i \tag{2}$$

3. Materials and methods

The samples used to evaluate the proposed method were 12 apples (6 from Red Delicious variety and 6 from Granny Smith variety), and 8 meat pieces (*semitendinosus* muscle). The CVS was a digital camera (Professional Series Network IP Camera Model 550710, Intellinet Active Networking, USA) connected to a PC (AMD Sempron 2200+, 768 MB RAM).

The volume of each sample was experimentally determined by liquid displacement method in a single measurement. The goodness of the developed FEM approach method was evaluated by comparison between experimental sample volume (V) and estimated volume ($\tilde{V}$) values of each reconstructed object. The parameters used for this aim were the percentage volume relative error (RE_V), the percentage volume mean absolute relative error ($MARE_V$) and the correlation coefficient (r). No experimental procedure was implemented to obtain actual values of the surface area, since the difficulty to manually measure this parameter.

$$RE_V(\%) = 100\ \frac{\tilde{V} - V}{V} \tag{3}$$

$$MARE_V(\%) = \frac{100}{N} \sum_{i=1}^{N} \left\| \frac{\tilde{V}_i - V_i}{V_i} \right\| \tag{4}$$

4. Results and discussion

4.1. Lofting technique

The CVS and the cut directions chosen for the samples are shown in Figures 1 and 2, respectively (see section 2.1). Image processing stages employed to approximate the boundary of slices are depicted in Figure 3. As can be seen, correct selection of background allowed performing a good segmentation process. This was translated in an accurate boundary approximation. Graphic results of object reconstruction and meshing over samples are shown in Figures 4 and 5. From visual inspection, the implemented technique correctly reproduced the shape of real food materials. The lofting method produced smooth and irregular surfaces, similar to the natural ones.

Since each contour of the cross-section segmented images consisted of a large number of data points, a small subset of those boundary points was used to construct a closed B-Spline curve, in order to obtain a simpler but still appropriated representation of the real boundary. To perform the lofting procedure, the number of points in such subset must be equal in all slices. The size of this subset influenced the accuracy of the lofting and subsequent FEM approach method. The amount of points in the subset is directly proportional to the approximation degree to the actual boundary. However, when the number of points was very large, since the boundary was represented digitally, (i.e. by pixels) the obtained B-Spline curve presented a sharp trajectory. These characteristics of the B-Spline curve are translated to the constructed NURBS surface and the computational requirements for the meshing step. Non smooth slices produced sharp surfaces (and solids), which involved a large amount of finite elements (Figure 6).

Another important feature of the skinning technique is the number of cross-sections used. As more slices were considered, best approximations to the real objects were obtained. However, in some cases where the modelled object presented smooth shape, the amount of cross-sections could be reduced, and so the computational costs. The applied slicing method presented one drawback: there existed a minimum thickness for the slices to obtain undamaged shape in cross-sections. This problem could be solved by using a non invasive slicing method, such as NMR (Nuclear Magnetic Resonance). This technique, widely used in medicine field, allows obtaining very thin slices without sample destruction in a fast and easy way. Also, recorded images present less experimental noise and high contrast between the sample and background, which is reflected in a better segmentation process. The main disadvantage of NMR method is its high cost and equipment availability. NMR technique is now being implemented and will be published in a future work.

Although the developed method is destructive and could be laborious, it needs not expensive laboratory equipment and it could be applied in another software environment. In addition, the method allows working with samples presenting high degree of irregularity. This is, objects wtih protrusions or cavities in surface, interior holes and shapes with very low sphericity. These kinds of morphological characteristics would be difficult to register using the non destructive methods previously reported, since they work with projections of the entire sample.

4.2. Volume and surface area estimation

The surface area and volume values of the reconstructed objects were calculated using Gaussian integration of 4th order. As was discussed above, a number of boundary points for slices representation must be selected. Therefore, an analysis of the influence of the size of boundary subset on surface area and volume estimation procedure was carried out. Several solids of one (representative) sample of meat piece were obtained using different point numbers in the boundary subset. The number of cross-sections was fixed to 11, the maximum obtained for the tested sample. As the number of considered boundary points was increased, the relative error when volume was estimated tended asymptotically to zero (Figure 7). For more than 33 boundary points, the estimation error was less than 1% (in absolute terms). Therefore, the size of the boundary subset was set to 33 points, for all tested samples, since low error was obtained and computational costs were acceptable.

Also, the effect of number of cross-sections in the approximation was analyzed using the same meat sample as above. For this aim, the first and last cross-sections were fixed and the intermediate cross-sections were successively included All solids were reconstructed using 33 points in the boundary subset of each slice. The same asymptotical behaviour as with boundary points was observed for the number of cross-sections (Figure 8). When this number was greater than 7, the estimation error of volume was lower than 1%.

When comparing the volume estimated by the FEM approach method with experimental results, high correlation was found for all tested samples (Figure 9). All results were summarized in Table 1. As can be seen, the FEM approach method provided results with low error dispersion being the mean estimation error less than 2% in absolute terms, in all cases. Also, mean relative error was calculated finding negative values: -1.25% for Granny Smith apple, -1.01% for Red Delicious apple, and -0.95% for meat pieces. These results indicated underestimation in volume prediction by FEM approach. Underestimation may be due to two facts: (i) the lofting technique uses a finite number of cross sections, therefore the reconstructed solid is an approximation to the real food; (ii) in spite of the use of curved simplices, these can not be highly distorted in order to follow the exact curvature of the real geometry, therefore a small part of the object is not filled with finite elements.

The developed FEM approach method exactly estimated the volume and surface area of objects formed with only planar faces, such as general polyhedrons (results not shown). In these cases, the finite elements used are straight, not distorted simplices, and the volume and surface area could be exactly predicted. Bearing in mind the good performance of the FEM approach method to estimate the volume of samples tested here, it is expected that the method can approximate the actual surface area of foodstuffs with high accuracy. So, to generalize the obtained results for each tested object, the estimated values of the surface area were correlated with the weight and volume of samples. For this aim, the following equations based on dimensional analysis (expressing *S*, *W* and *V* in terms of a characteristic length *L*) were proposed:

$$S = a_0 W^{2/3} \tag{5}$$

$$S = b_0 V^{2/3} \tag{6}$$

The fitting performance and the estimated parameter for the Eq. (5) and (6) are shown in Table 2. Both correlations fitted well the calculated surface area to experimental values of weight and volume, for all tested samples, as can be seen in Figure 10.

Prediction equations for surface area of apples reported by Clayton et al. (1995), obtained from experimental values (tape method), were compared against the FEM approach method results. Values of R^2 were 0.96 and 0.97, for Red Delicious and Granny Smith varieties, respectively. Also, Clayton et al. (1995) compared the experimental values with their FEM based method. They obtained R^2 values equal to 0.96 and 0.99, for Red Delicious and Granny Smith varieties, respectively. Furthermore, Eifert et al. (2006) reported an equation to predict the surface area of apples from weight measurement. It was a linear equation, with R^2 equal to 0.47. In the present work, Eq. (5) was obtained with R^2 greater than 0.93, in the apple cases.

5. Conclusions

The applied lofting technique allows obtaining an accurate representation of the real shape of irregular multi-dimensional foodstuffs. Furthermore, the developed FEM approach method demonstrated its ability to correctly predict volume and surface area of general objects, even presenting low symmetry and sphericity. The application of the resulting object reconstruction will be used as domain in simulation of preservation processes in a separate paper.

Nomenclature

$MARE_V$	volume mean absolute relative error (%)
r	correlation coefficient
RE_V	percentage volume relative error (%)
R^2	determination coefficient
S	surface area, cm^2
u	general scalar dependent variable
V	experimental volume, cm^3
$\tilde{V}$	estimated volume, cm^3
W	weight, g

Greek symbols

a_0	parameter of Eq. (5)

β_0 parameter of Eq. (6)

Acknowledgments

This research was supported by grants from CONICET, ANPCyT (PICT 2003/09-14677) and Universidad Nacional de La Plata from Argentina.

References

Beyer, M., Hahn, R., Peschel, S., Harz M., & Knoche, M. (2002). Analysing fruit shape in sweet cherry (*Prunus avium* L.). *Scientia Horticulturae, 96* (1-4), 139-150.

Clayton, M., Amos, N. D., Banks, N. H., & Morton, R. H. (1995). Estimation of apple fruit surface area. *New Zealand Journal of Crop and Horticultural Science, 23*, 345-349.

Cleland, D. J., Cleland, A. C., Earle, R. L., & Byrne, S. J. (1984). Prediction of rates of freezing, thawing or cooling in solids of arbitrary shape using the finite element method. *International Journal of Refrigeration, 7* (1), 6-13.

COMSOL AB. COMSOL *Multiphysics User's Guide*. Version: September 2005, COMSOL 3.2.

Crocombe, J. P., Lovatt, S. J, & Clarke, R. D. (1999). Evaluation of chilling time shape factors through the use of three-dimensional surface modelling. In *Proceedings of 20th International Congress of Refrigeration, IIR/IIF*, Sydney [Paper 353].

Currie, A. J., Ganeshanandam, S., Noiton, D. A., Garrick, D., Shelbourne, C. J. A., & Oraguzie, N. (2000). Quantitative evaluation of apple (*Mauls* x *domestica*

Borkh.) fruit shape by principal component analysis of Fourier descriptors. *Euphytica, 111*, 219-227.

Ding, W., Nesumi, H., Takano, Y., & Ukai, Y. (2000). Quantitative evaluation of the three-dimensional fruit shape and size of *Citrus* species based on spherical harmonic descriptors. *Euphytica, 114*, 103-115.

Du, C. J., & Sun, D. W. (2006). Estimating the surface area and volume of ellipsoidal ham using computer vision. *Journal of Food Engineering, 73* (3), 260-268.

Eifert, J. D., Sanglay, G. C., Lee, D.-J., Sumner, S. S., & Pierson, M. D. (2006). Prediction of raw produce surface area from weight measurement. *Journal of Food Engineering, 74* (4), 552-556.

Igathinathane, C., & Chattopadhyay, P. K. (1998a). Numerical techniques for estimating the surface areas of ellipsoids representing food materials. *Journal of Agricultural Engineering Research, 70* (4), 313-322.

Igathinathane, C., & Chattopadhyay, P. K. (1998b). On the development of a ready reckoner table for evaluating surface area of general ellipsoids based on numerical techniques. *Journal of Food Engineering, 36*(2), 233-247.

Igathinathane, C., & Chattopadhyay, P. K. (2000). Surface area of general ellipsoid shaped food materials by simplified regression equation method. *Journal of Food Engineering, 46* (4), 257-266.

Kumar, V. A., & Mathew, S. (2003). A method for estimating the surface area of ellipsoidal food materials. *Biosystems Engineering, 85* (1), 1-5.

Lee, D. J., Eifert, J. D., Zhan, P., & Westover, B. P. (2003). Fast surface approximation for volume and surface area measurements using distance transform. *Optical Engineering, 42*(10), 2947-2955.

Lee, D. J., Xu, X., Eifert, J. D., & Zhan, P. (2006). Area and volume measurements of objects with irregular shapes using multiple silhouettes. *Optical Engineering, 45*(2), 27202-27212.

Lin, C.-Y., Liou, C.-S., & Lai, J.-Y. (1997). A surface-lofting approach for smooth-surface reconstruction from 3D measurement data. *Computers in Industry*, *34*(1), 73-85.

Moustakides, G., Briassoulis, D., Psarakis, E., & Dimas, E. (2000). 3D image acquisition and NURBS based geometry modelling of natural objects. *Advances in Engineering Software, 31*(12), 955-969.

Piegl, L. (1991). On NURBS: a survey. *IEEE Computer Graphics and Application, 11*(1), 55-71.

Piegl, L., & Tiller, W. (1996). Algorithm for approximate NURBS skinning. *Computer-Aided Design*, *28* (9), 699-706.

Sabliov, C. M., Boldor, D., Keener, K. M., & Farkas, B. E. (2002). Image processing method to determine surface area and volume of axi-symmetric agricultural products. *International Journal of Food Properties*, *5*(3), 641-653.

Somsen, D., Capelle, A., & Tramper, J. (2004). Manufacturing of par-fried French-fries: Part 1: Production yield as a function of number of tubers per kilogram. *Journal of Food Engineering*, *61* (2), 191-198.

Taylor, M. A., Garboczi, E. J., Erdogan, S. T., Fowler, D. W. (2006). Some properties of irregular 3-D particles. *Powder Technology, 162*, 1-15.

Woodward, C. D. (1987). Cross-sectional design of B-Spline surfaces. *Computers and Graphics*, *11*(2), 193-201.

Woodward, C. D. (1988). Skinning techniques for interactive B-Spline surface interpolation. *Computer-Aided Design, 20* (8), 441-451.

Zheng, C., Sun, D. W., & Du C. J. (2006). Estimating shrinkage of large cooked beef joints during air-blast cooling by computer vision. *Journal of Food Engineering*, *72*(1), 56-62.

Table 1. Experimental volume values and estimated values of surface area and volume of samples.

	Number of cross sections	Average thickness of slices (mm)	Measured weight (g)	Measured volume (cm^3)	Estimated volume (cm^3)	Absolute relative error (%)	Estimated surface area (cm^2)	Density (g/cm^3)
Granny Smith Apple	14	5.6	227.4	295	289.37	1.91	221.29	0.771
	10	8.9	242.7	320	315.88	1.29	233.38	0.758
	11	8.2	265.2	360	347.10	3.58	248.07	0.737
	18	4.8	272.4	375	368.93	1.62	261.27	0.726
	18	4.9	280.1	380	375.38	1.22	261.91	0.737
	18	5.2	304.1	415	423.67	2.09	284.91	0.733
					$MARE_V$	1.95	Average density	
					r	0.9917		0.744
Red Delicious apple	13	5.6	211.5	260	249.63	3.99	200.98	0.813
	15	5.7	232.2	265	258.76	2.35	208.58	0.876
	15	5.7	235.7	275	273.92	0.39	216.43	0.857
	15	5.7	251.9	290	286.08	1.35	223.67	0.869
	15	5.9	286.5	330	334.70	1.42	243.92	0.868
	15	5.7	288.2	330	332.04	0.62	248.71	0.873
					$MARE_V$	1.69	Average density	
					r	0.9978		0.859
Meat pieces	10	12.8	494.5	470	458.36	2.48	401.56	1.052
	10	15	554.0	515	515.62	0.12	418.00	1.076
	10	16	579.1	550	553.89	0.71	428.07	1.053
	(*) 11	16	580.0	545	539.95	0.93	421.46	1.064
	12	13.1	594.5	565	547.21	3.15	437.73	1.052
	11	15	604.4	560	563.07	0.55	422.35	1.079
	13	12.6	758.3	705	706.74	0.25	498.35	1.076
	12	16	822.7	770	749.19	2.70	532.80	1.068
					$MARE_V$	1.36	Average density	
					r	0.9954		1.065

(*) Sample used to analyze the influence of cross-sections and boundary points numbers on the approximation error.

421 **Table 2.** Regression analysis data (Eq. (5)-(6)) between estimated surface area and

422 weight and volume measurements.

Sample	a_0	R^2	$ß_0$	R^2
Granny Smith apple	6.1117	0.9336	5.0085	0.9725
Red Delicious apple	5.6312	0.9828	5.0961	0.9582
Meat piece	6.1068	0.9460	6.3729	0.9644

423

424

Figure captions

Figure 1. Schematic representation of the employed computer vision system.

Figure 2. Schematic representation of the sectioning axis and slices for (a) apples and (b) meat pieces.

Figure 3. Example of the stages involved in image processing and boundary approximation over a meat slice. (a) Original RGB image of the transversal cut. (b) Grey-scale representation of the RGB image. (c) Grey-scale image histogram. (d) Binary image obtained by thresholding. (e) B-Spline approximation to a subset of binary image boundary points. (f) Original image and its approximated boundary.

Figure 4. Visual results of the reconstruction technique and meshing procedure applied to meat sample.

Figure 5. Visual results of the reconstruction technique and meshing procedure applied to Red Delicious apple.

Figure 6. Solids constructed by two apple slices, with different number of boundary points: (a) 33 boundary points; (b) 376 boundary points. Enlarged regions show in detail the smoothness of each solid.

Figure 7. Effect of boundary points number on reconstruction performance of a single representative meat sample. (a) Surface area (□, cm^2) and volume variation (◇, cm^3)

with number of boundary points. (b) Volume estimation error (○) as a function of boundary points number.

Figure 8. Effect of cross-sections number on reconstruction performance of a single representative meat sample. (a) Surface area (□, cm^2) and volume variation (◇, cm^3) with number of cross-sections. (b) Volume estimation error (○) as a function of cross-sections number.

Figure 9. Correlation between experimental and estimated volume values for reconstructed solids: (□) meat pieces; (△) Granny Smith apples; (○) Red Delicious apples.

Figure 10. Surface area variation with weight (a) and volume (b) of samples. (□) Meat pieces; (△) Granny Smith apples; (○) Red Delicious apples. Solid lines represent Eq. (5) and (6), in each case.

Fig 1:

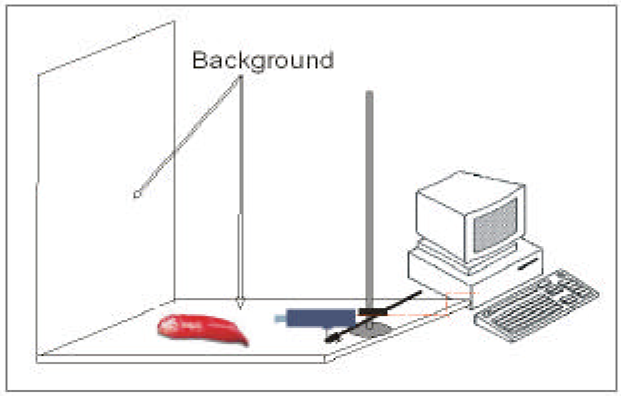

467 Fig 2:

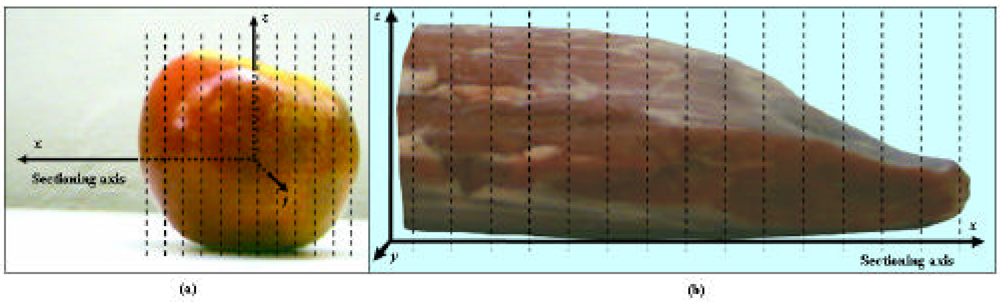

468

469 Fig 3:

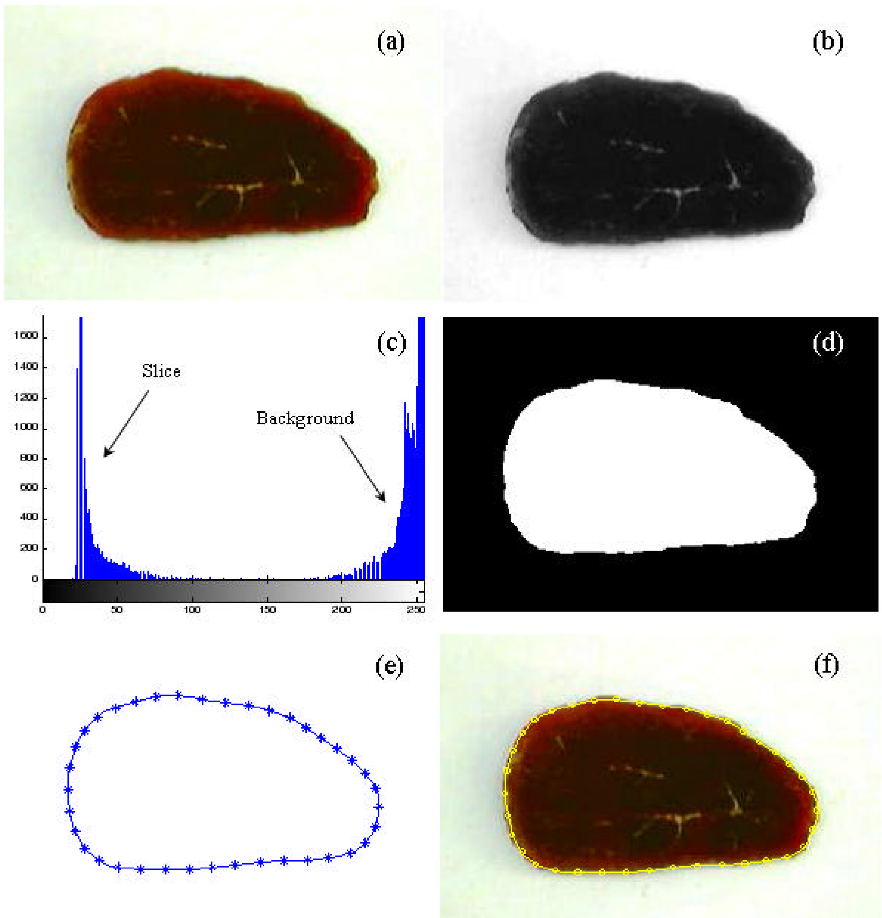

470

471 Fig 4:

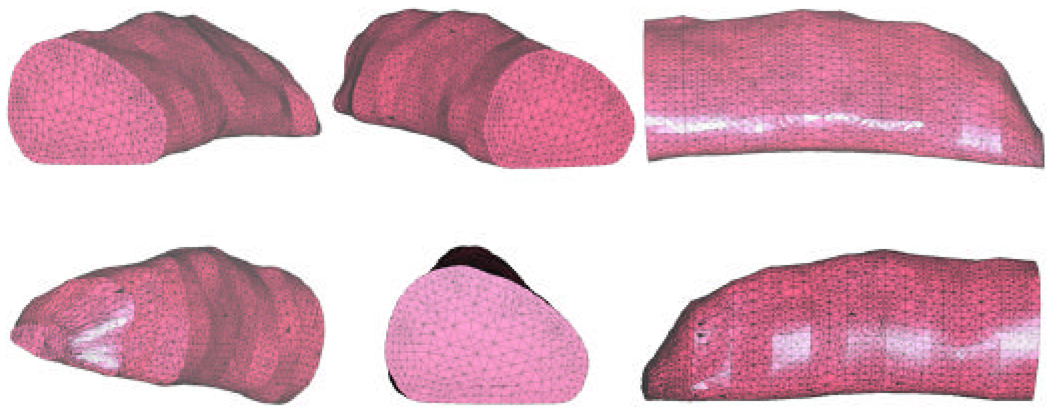

472

473 Fig 5:

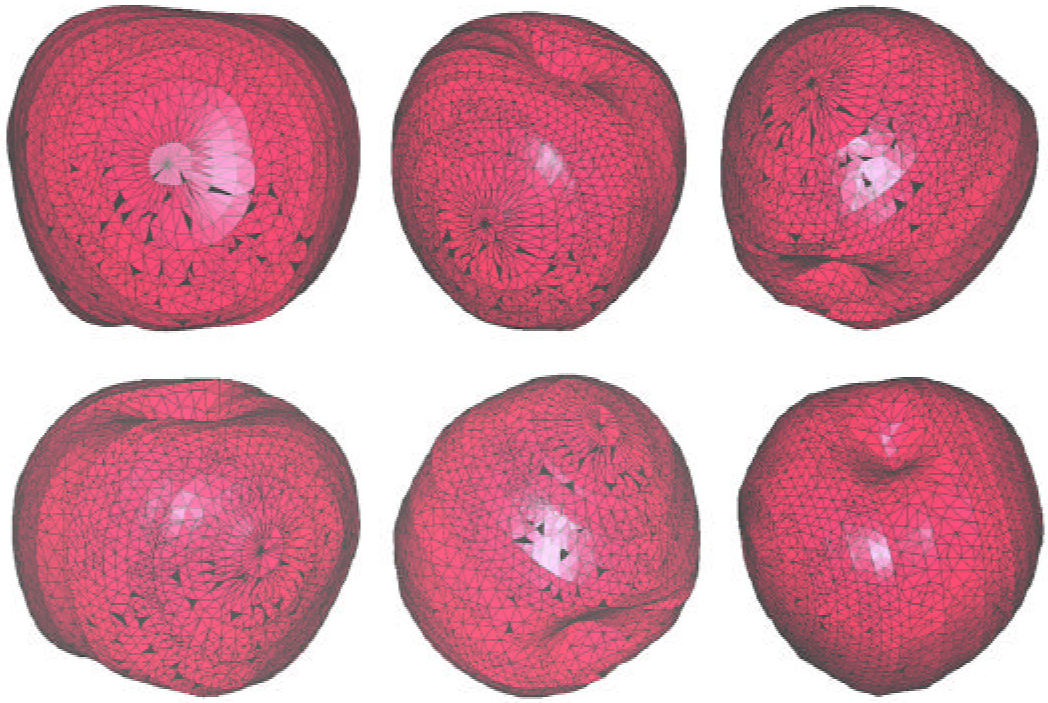

474

Fig 6:

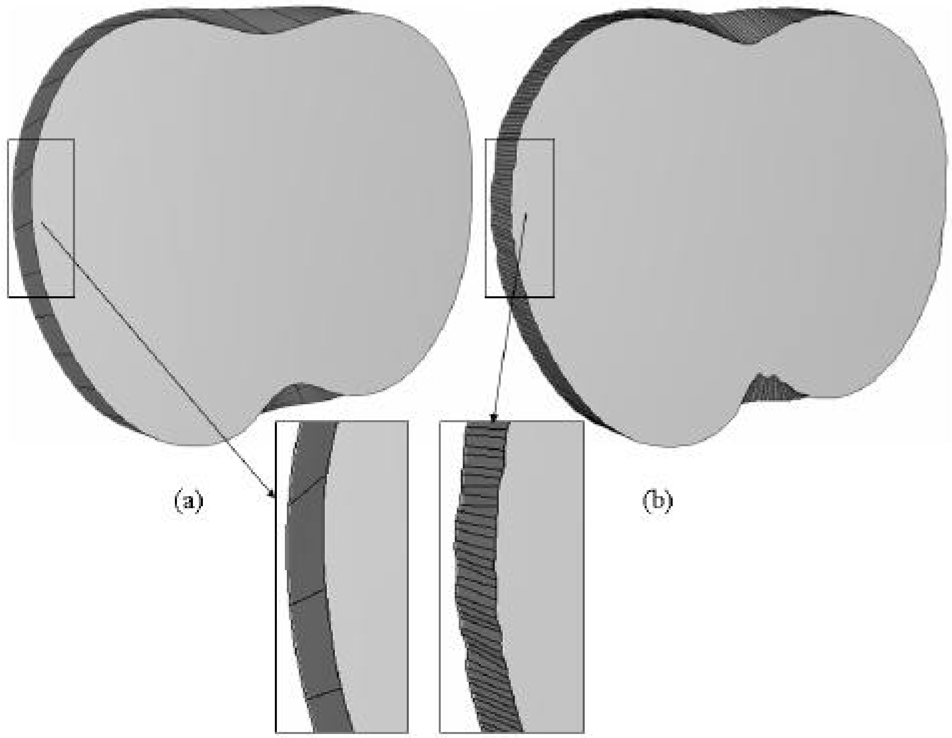

Fig 7:

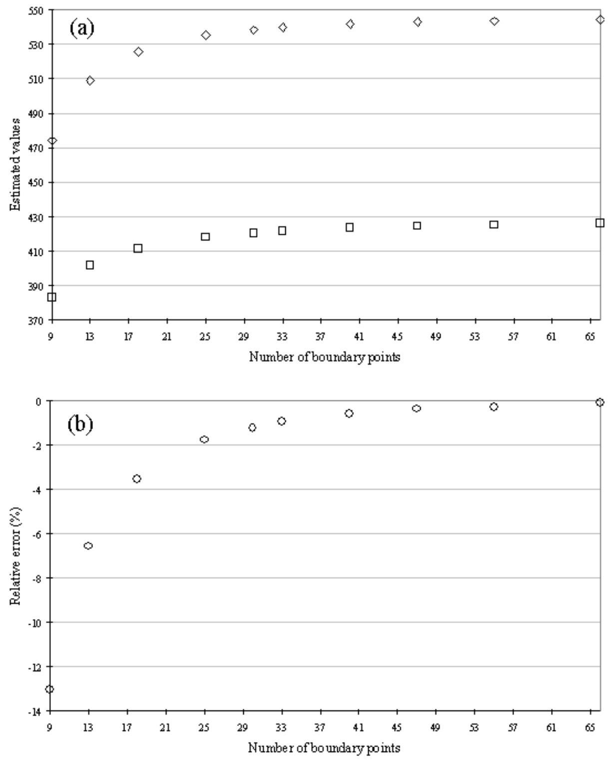
(a)
Estimated values
550
530
510
490
470
450
430
410
390
370
9
13
17
21
25
29
33
37
41
45
49
53
57
61
65
Number of boundary points
(b)
Relative error (%)
0
-2
-4
-6
-8
-10
-12
-14
Number of boundary points

Fig 8:

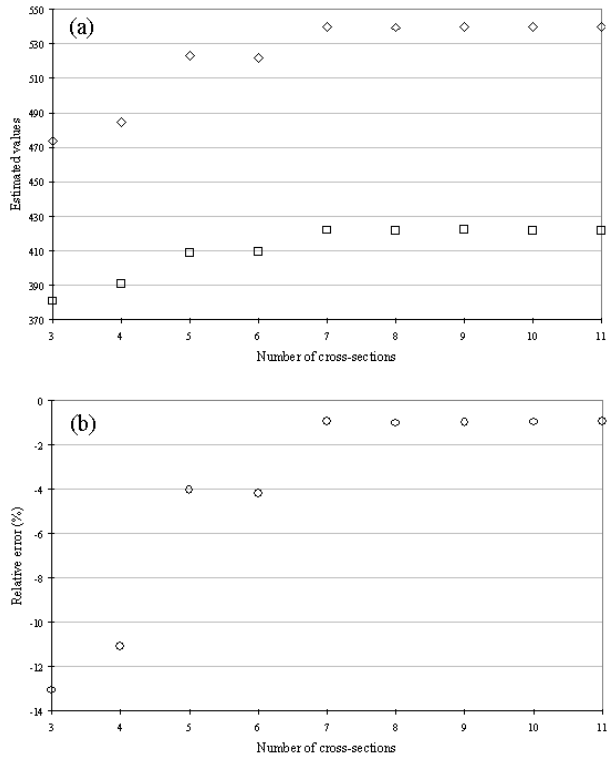
(a)
Estimated values
550
530
510
490
470
450
430
410
390
370
3 4 5 6 7 8 9 10 11
Number of cross-sections
(b)
Relative error (%)
0
-2
-4
-6
-8
-10
-12
-14
3 4 5 6 7 8 9 10 11
Number of cross-sections

481 Fig 9:

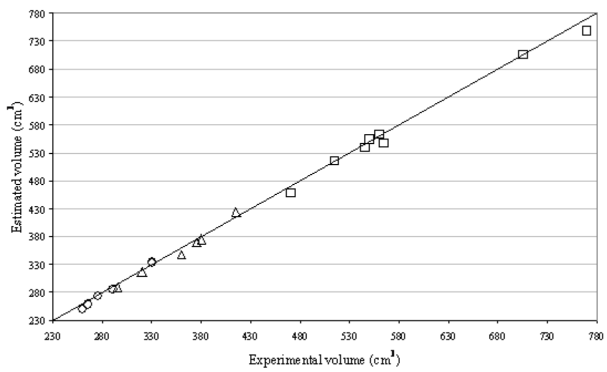
Estimated volume (cm³)
Experimental volume (cm³)
780
730
680
630
580
530
480
430
380
330
280
230
230
280
330
380
430
480
530
580
630
680
730
780

482

Fig 10:

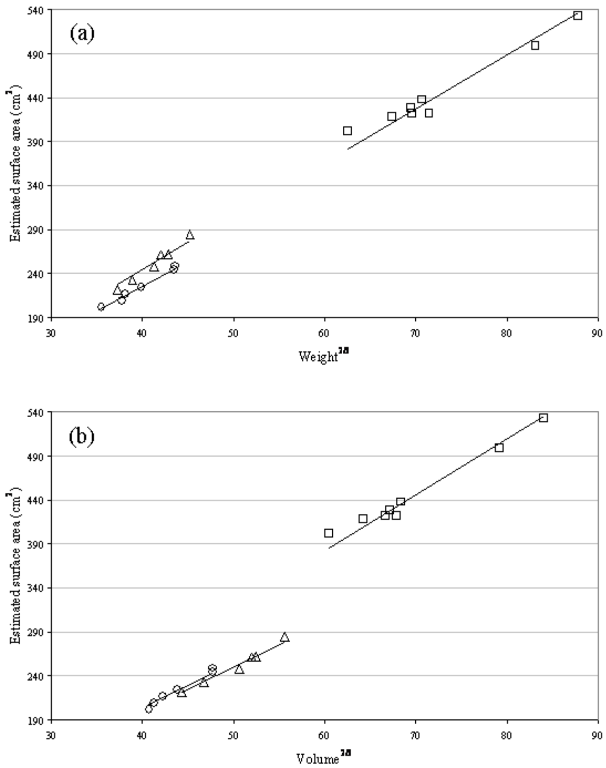
(a)
Estimated surface area (cm²)
Weight
(b)
Estimated surface area (cm²)
Volume